Mr. Manjunath Raikar. International Journal of Engineering Research and Applications
www.ijera.com
ISSN: 2248-9622, Vol. 11, Issue 8, August, 2021, pp: 48-54

RESEARCH ARTICLE OPEN ACCESS

166 kW Medium-Voltage Medium-Frequency Air-Core Transformer: Design and Experimental Analysis for 1:1-DCX Applications

Mr. Manjunath Raikar
Lecturer / Department of Electrical & Electronics
Sri Channakeshava Govt Polytechnic - Bankapur-581202, Dist Haveri
manjunathraikarn@gmail.com

Date of Submission: 01-08-2021 Date of acceptance: 11-08-2021

ABSTRACT
A medium-frequency (MF) magnetic-core transformer (MCT) is commonly used to achieve the galvanic isolation of solid-state transformers (SSTs). Previous demonstrations show that the design faces various obstacles to achieve extremely power dense and lightweight MCTs due to strict constraints related to cooling and insulation. This study looks at the potential efficiency of an air-core transformer (ACT) that has been designed to produce 166 kW at 7 kV. An ACT is the core portion of a DC Transformer (DCX), which is an unregulated DC-DC SST whose voltage scaling is determined by the transformer turns ratio. The ACT has a construction that is comparatively simple, has a high coupling value, and high efficiency. Guidelines for the insulation, cooling, and shielding of magnetic stray flux are covered in depth, along with an explanation of the modeling, optimization, and building of the realized ACT [3]. In addition, the prototype undergoes experimental validation to showcase its complete functioning. The achieved ACT in the analyzed DCX, which is based on a series resonant converter (SRC) architecture, is found to attain an unparalleled gravimetric power density of 16.5 kW/kg and a full-load efficiency of 99.5%. At 166 kW of output power, the whole DCX is predicted to achieve a 99% efficiency using 10 kV SiC MOSFETs.

Keywords: DC Transformer (DCX), air-core transformer (ACT), medium-frequency (MF), medium-voltage (MV), solid-state transformer (SSTs)

I. INTRODUCTION

The use of medium-frequency (MF) transformers, solid-state transformers (SSTs) offer galvanic isolation between two or more ports. At least one of these ports runs at medium-voltage (MV) levels, or voltages greater than one kV. Power outputs that are typically range from 50 kW to several megawatts. Due to these unique qualities, SSTs are an essential part of many new and developing applications, including future hybrid smart grid systems with AC and DC sections grid interfaces for renewable power sources [3], hyperscale data centers [5], high-power EV charging stations future ships [11], and future aircraft with distributed propulsion and on-board MVDC grids [12]. The medium-frequency transformer (MFT), which is the essential part of the SST, is commonly implemented as a magnetic-core transformer (MCT), ideally a dry-type MCT. However, the design of the MCT is difficult primarily due to strict cooling and insulating requirements, such as managing larger parasitic capacitances, void-free potting of the windings, and handling increased thermal resistances [15]. Moreover, the bulk of the dry-type insulation and magnetic cores restricts the possible gravimetric power density [9]. This is obviously a disadvantage for the aerial applications, but it may also make handling more difficult during manufacture and assembly in general.

The windings of air-core transformers (ACTs) must still be separated from one another but not from a magnetic core because, by definition, they do not have a magnetic core. This makes ACTs an intriguing substitute. This in turn makes it easier to employ air as a medium for insulation and to cool the windings directly at the same time. Therefore, ACTs have a very simple design and may attain high gravity power densities; one should anticipate a lower volumetric power density. Even though these systems usually use planar coils with relatively low coupling factors, recent publications show that high-power inductively coupled wireless power transfer (WPT) systems can achieve high efficiencies close to 99% and allow for overall DC-DC converter

efficiencies up to about 96% [13]. Such inductive power transfer (IPT) systems can achieve higher efficiency by multiplying the quality factor by the coupling coefficient. ACT designs for SST applications should be able to attain efficiencies significantly higher than 99% as different coil shapes with possibly greater coupling factors than planar coils (at similar quality factors) can be investigated for stationary applications. Furthermore, even though relatively high operating frequencies are required due to the low magnetizing inductance of an ACT, the realization of an ACT-based isolated DC-DC converter with an efficiency of close to 99%, which is a typical target efficiency for SSTs, seems feasible by utilizing available SiC power semiconductors that feature a high blocking voltage capability and a low on-state resistance.

In this work, an ACT—the essential part of a series resonant converter (SRC)—is analyzed. When an SRC is operated at its resonance frequency, it functions as a DC transformer (DCX) [6], strongly coupling the DC input and output voltages without requiring closed-loop regulation. Key specifications of the system are listed in Figure No.1,

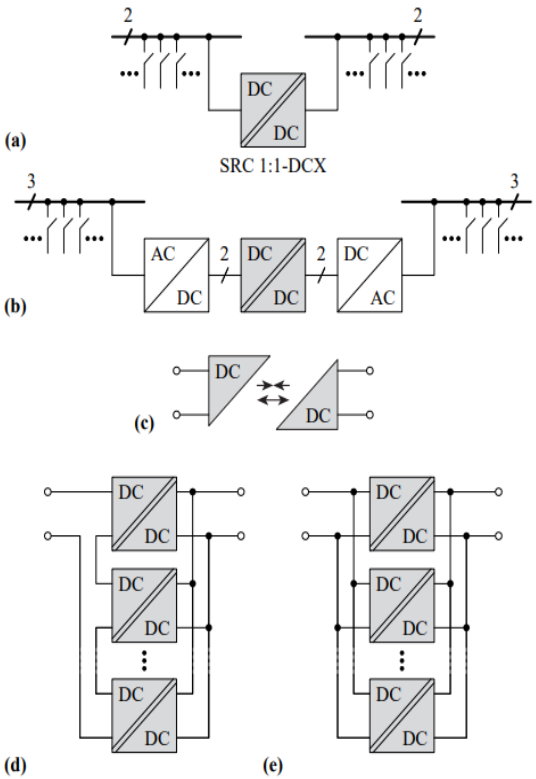

Figure No.1: DCX applications and options for scaling voltage and power ratings.

We take into consideration a 1:1-DCX ratio, which is ideal for several applications. For example, in DC bus-tie applications [11], the galvanic isolation of the 1:1-DCX allows for a more flexible grounding of subsystems than is possible with traditional switches or connectors. It guarantees equal bus voltages and unrestricted bidirectional power exchange in open-loop operation. Additionally, the 1:1-DCX may restrict output current or manage power flow, for example, by utilizing the quantum operating mode that was first described in [15]. The 1:1-DCX can be supplemented by AC-DC and DC-AC converters, which then take over the power flow regulation, to help with the connection of two AC grids [11] (see Fig. 1). Moreover, an ACT's lack of a magnetic core makes it possible to create contactless plugs, which eliminate sparks (see Fig. 1(c)). These plugs may be used in subsea applications or in other hostile or explosive settings, like mining.

Lastly, a 1:1-DCX enables simple, high-power back-to-back testing; that is, it allows the direct connection of the secondary side DC port to the primary side DC port. With this setup, the supply simply must cover the system's very small losses, allowing the system to be tested at high rated power levels [11]. Furthermore, as seen in Figure 1, several 1:1-DCX converters may be merged to adjust the total voltage or power rating, contingent on the use case. The main and secondary windings of the transformer would need a greater isolation voltage rating if the input series, output-parallel (ISOP) arrangement were to be used. An output-parallel, input-parallel (IPOP) setup with six 166 kW-1:1-DCX converters might be used to create a 1 MW system.

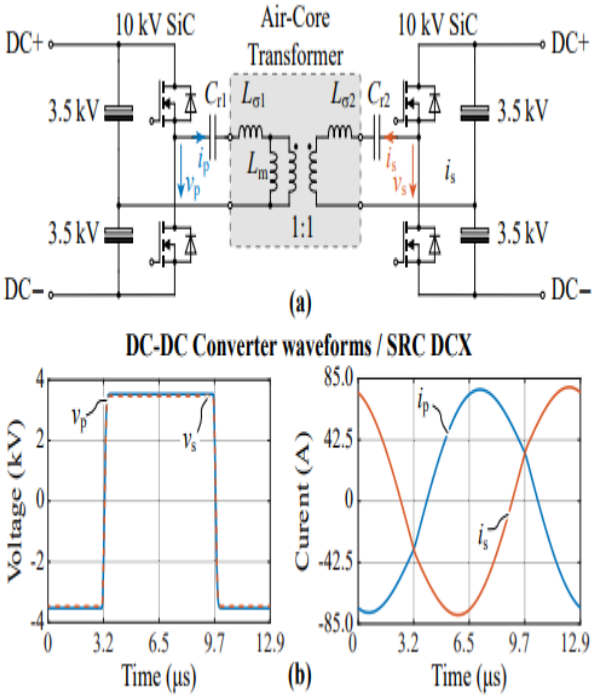

Figure No. 2: Converter topology of the 166 kW / 7 kV SRC 1:1-DCX

The 1:1-DCX converter's SRC structure and representative key waveforms are displayed in Fig. 2. To adjust the corresponding ACT stray inductances, Lσ1 and Lσ2, at the operating frequency, which is equal to the resonant frequency, the two series resonant capacitors, Cr1 and Cr2, are selected.

$$f_s = f_0 = \frac{1}{2\pi\sqrt{C_{r1}L_{\sigma 1}}}$$

This eliminates the requirement for closed-loop control and permits a tight coupling of the two DC bus voltages [6]. With a suitable margin for blocking voltage use, accessible 10 kV SiC MOSFETs may be used with the chosen DC bus voltage of 7 kV. Compared to a full bridge, the implementation using one half-bridge and one capacitive voltage divider per bridge only needs half as many switches [30]. Benefiting from well-defined voltages across the switches and magnetizing current that manifests in the primary and secondary side half bridges [22], the SRC converter has zero-voltage switching (ZVS) over the whole load range. In this regard, Section II of this study provides coil layouts for ACTs as well as general realization alternatives. After that, a thorough explanation of the modeling and multi-objective optimization of the 166 kW / 7 kV ACT is given in Section III. The actual hardware design of the optimized ACT is covered in Section IV. Information on the conductive shielding that reduces magnetic stray fields around the ACT and the isolation mechanism are also included. In Section V, we also carry out a comprehensive experimental investigation of the full-scale ACT prototype. In order to evaluate the effectiveness of the shielding, this comprises measurements of magnetic flux concentrations in the region of the ACT, calorimetric loss measurements, large-signal waveforms, and tiny signal measurements. Finally, the efficiency features of the ACT and the whole 1:1-DCX are covered in Section VI. With output power levels ranging from 25 kW to 166 kW, the realized ACT prototype achieves a measured efficiency of 99.5% and a gravimetric power density of 16.5 kW/kg. A rated output power of 99% may be achieved by the whole 1:1-DCX when 10 kV SiC MOSFETs are used.

II. PRIMITIVE CONFIGURATIONS FOR AIR-CORE TRANSFORMERS

One primary-side and one secondary-side coil, which can be assembled in a variety of ways, make up an ACT. To determine which realization option is best for additional optimization and design considerations, this part offers a succinct overview and a preliminary, qualitative evaluation of such possibilities. Furthermore, we provide the two fundamental approaches (i.e., using conductive or magnetic materials) for shielding against excessive magnetic stray fields.

2.1: Coil Arrangement

Planar coils, which are common for IPT/WPT systems [11], are used in a first promising configuration for the construction of an ACT (see Fig. 3). Many lateral coil forms, such as spiral [14], rectangular, or double-D [14], have been used. Planar coils are useful because they make it easier to find simple solutions for insulation and thermal control. To boost coupling and concurrently aid in shielding the magnetic stray flux, high-power IPT systems usually incorporate magnetic cores to steer the magnetic fields, primarily on the non-mating sides of the coils, to attain high efficiencies [12]. The possible gravimetric power density is restricted by the mass of the magnetic cores, which is a crucial factor for airborne applications and handling concerns in general. Although there is a dearth of literature on high-power air-core IPT systems—that is, planar coil configurations devoid of magnetic material—a similar 40 kW system was recently published in [32] and is notable for having a comparatively poor total DC-DC efficiency of about 90%. The absence of cores would necessitate the use of alternative methods for shielding the magnetic stray flux, even though for stationary applications such arrangements of planar coils can be expected to achieve higher coupling and hence higher efficiency than typical, mobility-oriented IPT/WPT systems (e.g., because a shorter air gap between the coils may be feasible).

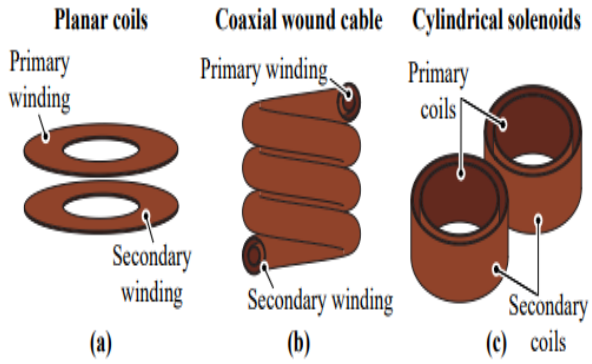

Figure No. 3: Considered coil arrangements for the ACT realization: (a) (spiral) planar coils; (b) coaxially wound cable in a solenoid arrangement; (c) cylindrical solenoids.

Most importantly, though, is that the bounding box geometry of planar IPT coil configurations is effectively limited to two degrees of freedom since they must be flat—that is, as power

transfer capability increases, the lateral dimensions get greater. As a result, the range of aspect ratios that may be used is limited, and some of the different ACT applications that were covered in the preceding section might not be appropriate for them.

Windings consisting of coaxial MV cable coiled onto a magnetic core have been proposed for MCTs with unity turns ratio and high isolation voltage requirements [5]– [7]. This configuration has the advantage of containing leakage flux inside the inter-winding space, which is the area between the coaxial cables metallic shield (secondary side winding) and core (primary side winding), which also naturally offers galvanic isolation. On the other hand, cooling the inner winding is more difficult and calls for a similarly intricate forced-air or liquid cooling system.

Furthermore, to generate a sufficiently high magnetizing inductance, an ACT in this design (see Fig. 3(b)) would need lengthy multi-turn coils [8]. We decided against pursuing this alternative further since it makes the production and cooling of the windings more difficult and requires that a relatively low coupling be assumed, even for a multi-turn coaxial cable ACT.

2.2: Coil Interconnection

Using two identical sets of two coaxially arranged coils, for example, with the inner coils connected in series to form the primary winding and the two outer coils connected likewise to form the secondary winding, would be a straightforward method to consider the interconnections of the four coils. The magnetic field for this case is simulated in two dimensions using the finite element method (FEM) in Fig. 4(a). Additionally, the extracted self-inductances of the primary-side winding, Lp, and the secondary-side winding, Ls, are asymmetric (basically because the diameters of the two primary-side coils are larger than those of the two secondary-side coils).

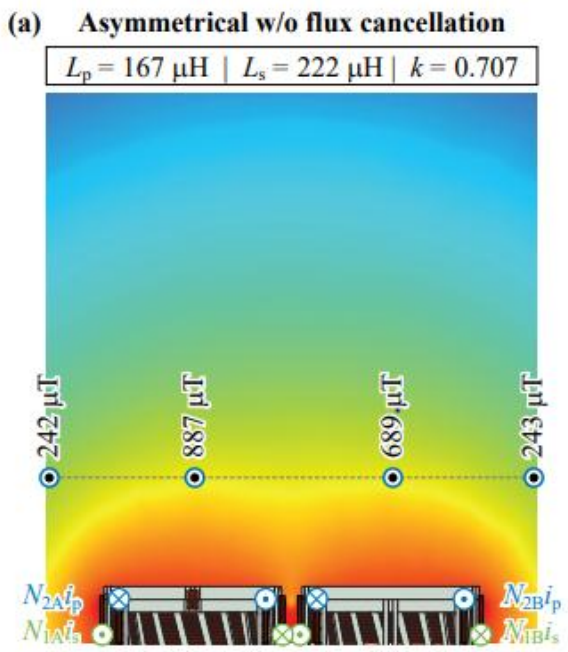

Figure No. 4: FEM-simulated flux densities within the cut plane defined

Consequently, Fig. 4(c) depicts a symmetric interconnection of the coils, with the primary- and secondary-side windings consisting of one outer and one inner coil each; that is, the primary-side winding is formed by the series connection of coils 1A and 2B, and the secondary-side winding is formed by the series connection of coils 1B and 2A (refer to Fig. 5 for the definitions of the coil identifiers). The winding directions also allow for partial stray flux cancellation, meaning that the average magnetic flux density over the points in the figure is 5% higher for the asymmetrical configuration with flux cancellation from Fig. 4(b) but approximately 25% lower for the symmetrical case compared to the asymmetrical interconnection without flux cancellation from Fig. 4(a). However, symmetrical self-inductances have important system-level advantages. For example, because the 1:1-DCX is symmetric, it can function with the same series resonant capacitance values on both sides of the transformer, making it easier to construct using standardized building blocks like resonant capacitor banks.

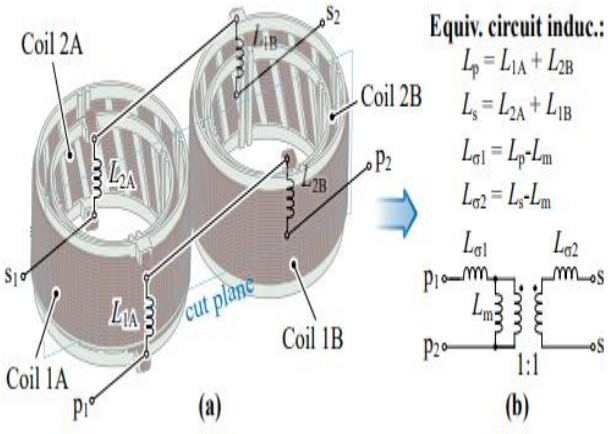

Figure No. 5 - CAD rendering showing the selected coil arrangement

For the following study of the MV/MF ACT, we thus take into consideration two coaxially arranged, cylindrical primary- and secondary-side windings and the symmetrical coil interconnection technique; see Fig. 5, which also depicts the corresponding lossless linear equivalent circuit. The two leakage inductances, Lσ1 ≈ Lσ2, are symmetrical because the primary- and secondary-side self-inductances, Lp ≈ Ls, are both symmetrical.

III. DESIGN AND CONSTRUCTION

The geometry of the active part of the ACT is determined by the Pareto optimization discussed in the previous section. A few other factors, such as the isolation coordination, cooling, and airflow, and the practical implementation of an appropriate conductive shielding, influence the mechanical design of the prototype. In terms of the overall mechanical configuration, Fig. 8(a) illustrates how, to expedite manufacture, each coil's single-layer winding is positioned on a separate 3D-printed polycarbonate coil former.

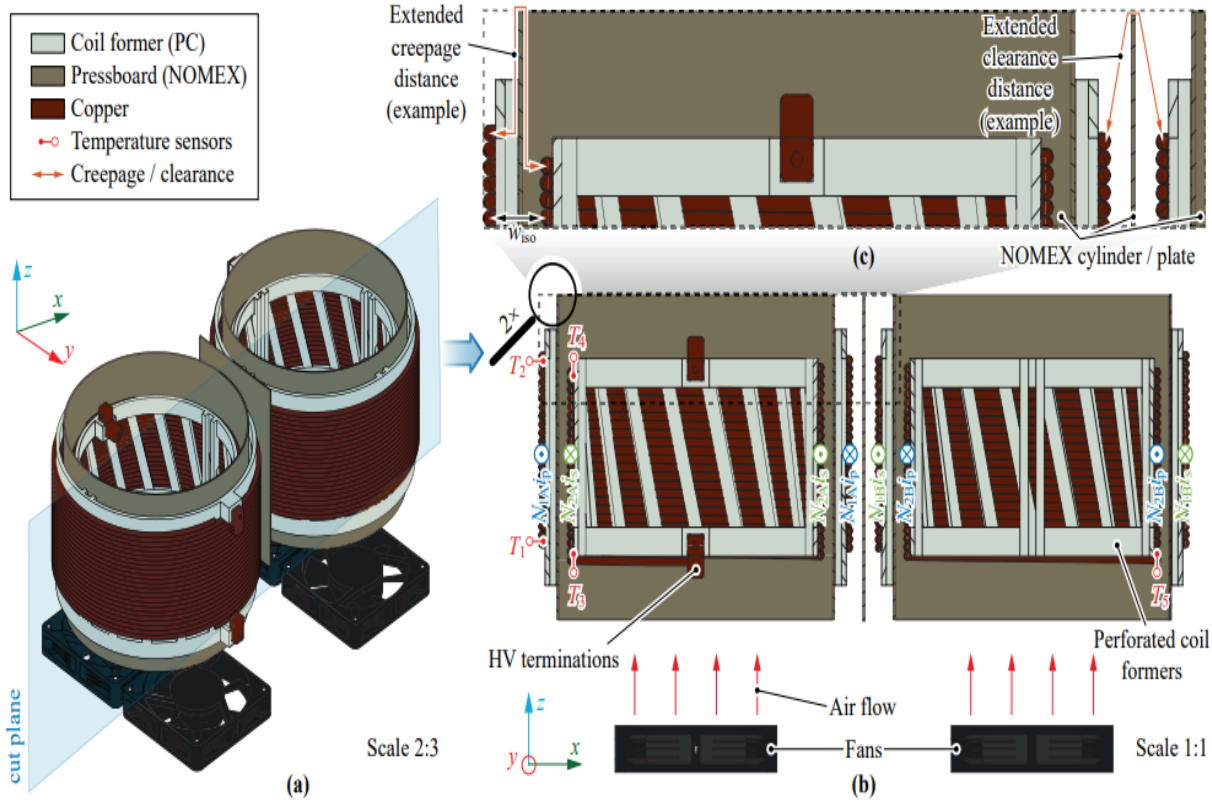

Figure No. 6 - A simplified perspective of the three-dimensional transformer model displaying the insulating barriers, fans, coil formers, windings, and terminations.

We consider design clearance and creepage distances in accordance with IEC 62477, and a rated DC isolation voltage of Vi = 10 kV, i.e., with some reserves beyond the rigorous functional requirement of the 7 kV DC bus voltage. For overvoltage category III (OV-III), which requires an impulse withstand voltage of 37 kV, the minimum necessary clearance distance consequently becomes 55 mm. Likewise, considering isolation material group II and pollution degree 2 (PD2), the minimum

necessary creepage distance is 71 mm. The primary and secondary-side coils of a NOMEX pressboard are separated by cylindrical barrier elements with a thickness of 1.5 mm, and a rectangular NOMEX plate with a thickness of 1.5 mm is positioned between the two sets of coils to achieve this clearance and creepage distances (see Fig. 8(c)). It is possible to extend the clearance (66 mm), which corresponds to an impulse withstand voltage of about 43 kV, and the creepage (79 mm) beyond the minimal values without affecting other elements of the mechanical design.

It should be noted that the standard requires larger clearance lengths for high-altitude applications (over 2 km above sea level) due to the reduced air pressure. For example, the DO160 G standard's A1 category for airborne equipment calls for operation in environmentally protected (pressurized) zones up to 4.6 km (15, 000 ft). This means that, in accordance with IEC 62477, the clearance lengths must be increased by a factor of 1.4. By lengthening the NOMEX barrier components, the clearance (and creepage) lengths of the proposed ACT may be readily increased to satisfy such criteria, in contrast to standard MCTs. The cautious measurement of the maximum electric field between the primary-side and secondary-side coils lends credence to this.

IV. CONCLUSION

This work presents the design, implementation, and experimental assessment of an air-core transformer (ACT) with a capacity of 166 kW and a voltage of 7 kV. The transformer is a component of a DC transformer (DCX), which is the DC-DC converter stage of a solid-state transformer (SST). With two sets of coaxially arranged solenoids, the realized full-scale prototype of the MV/MF ACT achieves a remarkably high coupling factor of 0.76. This construction leads to a partial elimination of magnetic stray flux and a symmetrical arrangement of the primary and secondary side windings. Since air can be used as both a cooling medium and an insulating material, the actualization of the ACT is relatively simple. As a result, the corresponding difficulties associated with conventional magnetic-core transformers (MCTs)—such as void-free potting of the windings, partial discharges, and dielectric losses—are avoided. Additionally, because a sizable portion of the transformer coils may be cooled by forced air, the thermal design is made simpler. Consequently, a winding current density of greater than 7 A/mm2 may be used to run the ACT.

Additionally, operation at up to 70% of the rated power is possible while using passive cooling, or natural convection, such as when a fan is malfunctioning. These factors result in very easy and hence affordable manufacture, which is enhanced by easier handling due to the comparatively small bulk. The nominal insulation voltage of the ACT prototype is 10 kV. The IEC 62477 clearance and creepage distances are achieved by filling the air spaces between the primary and secondary side windings using barrier components composed of NOMEX. Unlike MCTs, the barrier elements' length can be simply extended to increase the clearance and creepage distances. This allows the elements to be customized to meet more stringent requirements, such as those for airborne applications, where longer clearance distances are required to account for lower air pressure. To lower the magnetic stray flux around the transformer, a conductive shielding shell made of aluminum is developed, constructed, and tested. The ICNIRP 2010 requirements governing the magnetic stray flux levels for public exposure at 200 mm from the shielding are satisfied by the proposed shielding, making the ACT complaint. By adding the shielding enclosure, the transformer's weight increases by around 10%, its overall losses decrease by 6%, and its boxed volume is determined. This results in a volumetric power density of 2.2 kW/dm3, which is lower than the 7.8 kW/dm3 it would have without the shielding.

REFERENCE

[1]. J. E. Huber and J. W. Kolar, “Applicability of Solid-State Transformers in Today’s and Future Distribution Grids,” IEEE Trans. Smart Grid, vol. 10, no. 1, pp. 317–326, Jan. 2019.

[2]. T. Dragicevic, J. C. Vasquez, J. M. Guerrero, and D. Skrlec, “Advanced LVDC Electrical Power Architectures and Microgrids: A Step Toward a New Generation of Power Distribution Networks.” IEEE Electrific. Mag., vol. 2, no. 1, pp. 54–65, Mar. 2014.

[3]. P. C. Kjaer, Y.-H. Chen, and C. G. Dincan, “DC Collection: Wind Power Plant with Medium Voltage DC Power Collection Network,” presented at the ECPE Workshop Smart Transf. Traction Future Grid Appl., Zurich, Switzerland, 2016.

[4]. S. Falcones, R. Ayyanar, and X. Mao, “A DC–DC MultiportConverter-Based Solid-State Transformer Integrating Distributed Generation and Storage,” IEEE Trans. Power Electron., vol. 28, no. 5, pp. 2192–2203, May 2013.

[5]. S. Srdic and S. Lukic, “Toward Extreme Fast Charging: Challenges and Opportunities in Directly Connecting to

Medium-Voltage Line," IEEE Electrific. Mag., vol. 7, no. 1, pp. 22–31, 2019.

[6]. H. Tu, H. Feng, S. Srdic, and S. Lukic, "Extreme Fast Charging of Electric Vehicles: A Technology Overview," IEEE Trans. Transport. Electrific., vol. 5, no. 4, pp. 861–878, Dec. 2019.

[7]. S. Castellan, R. Menis, A. Tessarolo, and G. Sulligoi, "Power Electronics for All-Electric Ships with MVDC Power Distribution System: An Overview," in Proc. of Int. Conf. on Ecological Vehicles and Renewable Energies (EVER), 2014, pp. 1–7.

[8]. G. Ulissi, S.-Y. Lee, and D. Dujic, "Solid-State Bus-Tie Switch for Shipboard Power Distribution Networks," IEEE Trans. Transport. Electrific., vol. 6, no. 3, pp. 1253–1264, Sep. 2020.

[9]. N. Madavan, "NASA Investments in Electric Propulsion Technologies for Large Commercial Aircraft," in Proc. of Electric and Hybrid AerospaceTechnology Symposium, 2016.

[10]. P. Czyz, T. Guillod, F. Krismer, and J. W. Kolar, "Exploration of the Design and Performance Space of a High Frequency 166 kW/10 kV SiC Solid-State Air-Core Transformer," in Proc. of the IEEE Int. Power Electron. Conf. (ECCE Asia), 2018, pp. 396–403.

[11]. M. Armstrong, "Superconducting Turboelectric Distributed Aircraft Propulsion," in Proc. of Cryogenic Engineering Conf. / Int. Cryogenic Materials Conf., 2015.

[12]. T. Guillod, R. Faerber, D. Rothmund, F. Krismer et al., "Dielectric Losses in Dry-Type Insulation of Medium-Voltage Power Electronic Converters," IEEE Trans. Emerg. Sel. Topics Power Electron., vol. 8, no. 3, pp. 2716–2732, Sep. 2020.

[13]. M. Mogorovic and D. Dujic, "100kW, 10kHz Medium Frequency Transformer Design Optimization and Experimental Verification," IEEE Trans. Power Electron., vol. 34, no. 2, pp. 1696–1708, May 2019

[14]. Gammeter, F. Krismer, and J. W. Kolar, "Comprehensive Conceptualization, Design, and Experimental Verification of a WeightOptimized All-SiC 2 kV/700 V DAB for an Airborne Wind Turbine," IEEE Trans. Emerg. Sel. Topics Power Electron., vol. 4, no. 2, pp. 638–656, Jun. 2016.

[15]. G. B. Joung, C. T. Rim, and G. H. Cho, "Modeling of Quantum Series Resonant Converters-Controlled by Integral Cycle Mode," in Proc. Of the IEEE Industry Appl. Society Annual Meeting, 1988, pp. 821–826.